

Shear-induced diffusivity in supercooled liquids

Mangesh Bhendale¹, Jayant K. Singh¹, and Alessio Zaccone^{2*}

¹Department of Chemical Engineering, Indian Institute of Technology Kanpur, 208016 Kanpur, India. and

²Department of Physics “A. Pontremoli”, University of Milan, via Celoria 16, 20133 Milan, Italy.

The Taylor-Aris theory of shear diffusion predicts that the effective diffusivity of a tracer molecule in a sheared liquid is enhanced by a term quadratic in the shear rate. In sheared supercooled liquids, instead, the observed enhancement is linear in the shear rate. This is a fundamental observation for the physics of nonequilibrium liquids for which no theory or fundamental understanding is available. We derive a formula for the effective molecular diffusivity in supercooled liquids under shear flow based on the underlying Smoluchowski equation with shear (Smoluchowski diffusion-convection equation) with an energy barrier representing a crowded energy landscape. The obtained formula correctly recovers the effective diffusivity with a correction term linear in the shear rate, in agreement with results from numerical simulations of different liquids as well as with earlier experimental results on shear melting of colloidal glass. The theory predictions are supported by comparisons with molecular simulations of supercooled water and supercooled Lennard-Jones liquids, which confirm that the predicted enhancement of diffusivity is inversely proportional to temperature and directly proportional to the zero shear viscosity.

The celebrated Taylor-Aris theory [1, 2] of diffusion in a liquid undergoing shear flow (e.g. pipe flow) provides a foundation for understanding a variety of chemical and biochemical processes which occur in capillary flow as well as in industrial and environmental flows. The Taylor-Aris theory is based on solving the diffusion-convection equation for a tracer particle in the absence of any conservative force-field or potential energy landscape (PEL). It provides a formula for the effective diffusivity enhanced by the shear flow given by:

$$D_{\text{eff}} = D \left(1 + \frac{Pe^2}{48} \right) \quad (1)$$

where $Pe = R\bar{w}/D$ is the Peclet number, with R the pipe radius, $\bar{w} \propto \dot{\gamma}$ is the average flow velocity in the pipe with $\dot{\gamma}$ the shear rate, and D is the molecular diffusivity of the tracer particle in the absence of flow.

In contrast with this result for a free diffusing molecule or particle in shear flow, the effective diffusivity measured experimentally or in numerical simulations in *supercooled* liquids under shear flow, reads as [3–5]

$$D_{\text{eff}} = D (1 + c\dot{\gamma}) \quad (2)$$

for some constant c independent of shear rate $\dot{\gamma}$. Hence, in supercooled liquids, the effective diffusivity is enhanced by a term which is linear in the shear rate, contrary to the Taylor-Aris result (valid for non-supercooled liquids) where the dependence on the shear rate is quadratic. This is a fundamentally unsolved problem in the statistical mechanics of nonequilibrium liquids [6].

In the following, we provide the first physical derivation of Eq. (2) based on the solution to the Smoluchowski diffusion-convection equation with a potential

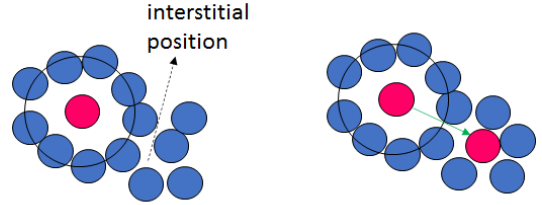


Figure 1. Schematic illustration of an event by which a particle abandons its original quasi-equilibrium position in the cage formed by its nearest-neighbours and jumps under the influence of thermal fluctuations to a new quasi-equilibrium position just outside the cage. The energy barrier V_{max} can be estimated as the elastic energy needed to accommodate the particle in the cavity, which for simplicity is taken to be spherical. This leads to a quantitative estimate of V_{max} [8].

barrier representing the glassy cage in the supercooled liquid.

The starting point is the Frenkel theory of diffusivity in a potential energy landscape [7]. In a crowded fluid, such as a supercooled liquid, the controlling process is the thermally activated hopping of a tagged molecule which escapes from the cage of its nearest-neighbors, Fig. 1.

From an energy-landscape perspective, this is a barrier-crossing process with a characteristic time-scale τ , which typically is an Arrhenius function of the characteristic energy barrier V_{max} . This energy barrier can be related, via the shoving model, to the high-frequency elastic modulus [8, 9] and/or to the underlying glassy dynamics via mode-coupling type approaches [10].

According to Frenkel, the diffusivity of a particle (atom, molecule) in an energy landscape is given by [7]:

$$D = \frac{\delta^2}{6\tau} \quad (3)$$

where δ is the characteristic length-scale of the barrier-crossing process, typically of the order of the cage size

* alessio.zaccone@unimi.it

(cfr. Fig. 1), hence 2-3 times the particle diameter.

In the absence of shear flow, the hopping time scale for the particle to diffuse out of the cage is evaluated via the Kramers method considering an energy barrier set by the cooperative slowing down predicted e.g. by mode-coupling theory [10]. In the presence of shear, the dynamics is described by the many-body Smoluchowski equation with shear [11]. Since we are interested in the shear-rate dependence, we assume the existence of a many-body potential barrier which arises from the glassy dynamics [10]. In terms of the (static) pair correlation function $g(r)$, this can be written as a potential of mean force [12]: $V(r) = -k_B T \ln g(r)$. In this picture, the tagged particle experiences an attractive potential well corresponding to the first peak in the $g(r)$ followed by an energy barrier corresponding to the first minimum in the $g(r)$, spatially represented by the glassy cage [13].

Under these conditions, the dynamics of the tagged particle in the presence of drift terms, is governed by the Smoluchowski diffusion equation with shear [14–17] for the probability density function (pdf) ρ of finding the tagged particle at a position \mathbf{r} :

$$\frac{\partial \rho}{\partial t} + \nabla \cdot [-D_0 \nabla \rho + \mathbf{K} \rho] = 0 \quad (4)$$

where D_0 is the single-particle diffusion coefficient in the high-temperature (not supercooled) liquid. In the above, \mathbf{K} is the generalized drift, which contains the drift due to the PEL and that due to the shear flow [16]. By the definition of the stationary current \mathbf{J} , we recover the continuity equation $\partial \rho / \partial t + \nabla \cdot \mathbf{J} = 0$. At steady-state, the continuity equation dictates that the stationary current of probability density over a spherical surface is $J = 4\pi r^2 (-D_0 \partial \rho / \partial r + K_r \rho)$, where K_r is the radial component of the drift field \mathbf{K} .

Let \hat{r} be the unit vector measured from the center of the tagged particle along the outward trajectory. Clearly, only the current along this (positive) direction matters for the calculation of the barrier-crossing time τ . The drift term in the presence of both an underlying PEL and an external flow reads as $K_r = -b(\partial V / \partial r) + b v_r$. One should note that in the convection-diffusion equation studied by Taylor [1] and Aris [2] the PEL term $-b(\partial V / \partial r)$ is absent. Here $v_r \equiv \mathbf{v} \cdot \hat{r}$ is the radial component of the velocity due to the imposed shear flow. The spherically-averaged, radial current becomes [18]

$$J = 4\pi r^2 \left(-D_0 \frac{\partial \rho}{\partial r} - b \frac{\partial V}{\partial r} \rho + b v_r \rho \right). \quad (5)$$

In polar coordinates we integrate over all angles to find this radial current across a spherical cross section. However, only those regions of the solid angle where the flow drives the particle over the barrier of the glassy cage matter for the calculation of τ . These regions correspond to regions of solid angle where v_r is positive, whereas the regions where v_r is negative do not contribute [18].

Without loss of generality, we consider simple shear flow given by $\mathbf{v}(x, y, z) = \dot{\gamma}[y, 0, 0]$ (other flow geometries can be implemented which is going to affect only

a numerical prefactor in the final result). Under the assumption of weak-coupling between the flow field and the density field, $\rho(r)$ and v_r are relatively uncorrelated over the solid angle (one should recall that v_r also depends on the polar angle of the vector \hat{r}). This approximation has been checked by numerics in Ref. [16] and shown to be able to yield reasonable results also for intense flows. Hence, $\langle \rho v_r \rangle \approx \langle \rho \rangle \langle v_r \rangle$, where the $\langle \dots \rangle$ indicates the angular average restricted to the regions of the solid angle where the flow velocity acts as to move the particle at the center of the cage outwardly over the cage, i.e. where $v_r > 0$. This is done always considering a spherical frame centered on the tagged particle at the center of the cage. In general, we have [14]

$$\begin{aligned} \langle v_r \rangle &= \frac{1}{4\pi} \int_{\Omega} \dot{\gamma} r \sin^2 \theta \sin \phi \cos \phi \sin \theta d\theta d\phi \\ &= \frac{1}{3\pi} \dot{\gamma} r. \end{aligned} \quad (6)$$

To obtain the result in the second line, the angular integral is taken over the restricted set Ω of regions in the solid angle where the radial component of the flow velocity (and the associated drift) is positive along \hat{r} [18], thus pushing the particle away from the center of the cage over the barrier. For a different flow geometry, axisymmetric extensional flow, one would get $\langle v_r \rangle = \dot{\gamma} r / (3\sqrt{3})$ [18].

With an exact algebraic manipulation, we can rewrite Eq.(5) as [19, 20]

$$J = -4\pi r^2 D_0 e^{-V_p/k_B T} \frac{d}{dr} \left[e^{V_p/k_B T} \rho \right] \quad (7)$$

where $V_p \equiv \int_0^r K_r ds$ is the primitive integral of the generalized drift K_r introduced above. Following the Kramers' method [21], we integrate Eq. (7) between r^* , a generic point near the cage center (corresponding to a point of minimum in the PEL $V(r)$), and C . Here C is some point sufficiently away on the radial axis beyond the cage, more precisely it can be identified with the second maximum in the $g(r)$, i.e. with the second minimum in $V(r) = -k_B T \ln g(r)$ [13]. Since the probability density becomes much smaller at $r = C$, we can express the steady current as

$$J = \frac{e^{V_p(r^*)/k_B T} \rho(r^*)}{a^{-2} \int_{r^*}^C \frac{e^{V_{\text{eff}}(r)/k_B T}}{4\pi D} dr} \quad (8)$$

where the effective potential is given by

$$V_{\text{eff}}(r) \equiv V(r) - b \int_0^r \langle v_r \rangle s^2 ds - 2k_B T \ln(r/a). \quad (9)$$

This effective potential maps our 3D problem onto an effectively 1D problem but leaves the physics unaltered. The logarithmic term is necessary to recover the metric factor r^{-2} in the integral of Eq. (8), such that one can recover Eq. (5) upon going backwards in the transformation [22]. The integral in Eq.(8) is indefinite, because it is the primitive integral (antiderivative), and the integration constant is chosen equal to

zero such that we recover the case with no flow when $v_r = 0$. The steady-state probability density inside the attractive well at the center of the cage is given by the stationary-state shear-distorted distribution ρ_{st} by means of the quasi-steady state approximation in the well [18], $\rho_{st}(r) = \rho(r^*)e^{-[V_p(r)-V_p(r^*)]/k_B T}$ (this is simply the form which solves the steady-state time-independent limit of Eq. (4)).

Thus the probability of finding the particle in the 3D well centered at the center of the cage is given by integrating the density over a spherical shell of this well,

$$\rho_{st} = \rho(r^*)e^{V_p(r^*)/k_B T} a^2 \int_A^B e^{-V_{\text{eff}}(r)/k_B T} 4\pi dr \quad (10)$$

where A is a point slightly to the left of the PEL minimum (i.e. to the left of the cage center), and B is a point slightly to the right [21]. Upon taking $C \rightarrow \infty$, the mean first-passage time across the barrier is given by the Kramers theory [21, 23] as $\tau = \rho_{st}/J$. Using the standard saddle-point method [21] to approximate the integrals analytically to quadratic order both near the well bottom and near the barrier top in the integrals appearing in ρ_{eq} and J , respectively, we obtain the time-scale for the shear-assisted crossing of the PEL cage barrier:

$$\tau = \frac{2\pi b \exp[\beta V_{\text{eff}}(r_{\text{max}}) - \beta V_{\text{eff}}(r_{\text{min}})]}{\sqrt{-V''_{\text{eff}}(r_{\text{max}})V''_{\text{eff}}(r_{\text{min}})}}, \quad (11)$$

where r_{min} and r_{max} represent the coordinates of the minimum and maximum in $V_{\text{eff}}(r)$ and $\beta = 1/(k_B T)$.

Upon substituting Eq. (6) in Eq. (9), and then the latter in Eq. (11), we obtain:

$$\tau = \frac{2\pi b \exp[\beta V(r_{\text{max}}) - \beta V(r_{\text{min}})]}{\sqrt{-V''(r_{\text{max}})V''(r_{\text{min}})}} e^{-\beta b \dot{\gamma} \Delta r^2 / 6\pi}, \quad (12)$$

where we separated the contribution due to the shear flow from that which survives in the limit of zero shear. Here, Δr represents the spatial distance between the final position of the particle outside the cage and its original position at the center of the cage, hence $\Delta r \sim 2\sigma = 4a$, with reference to the right panel in Fig. 1. Since the shear velocity is linear in r , it does not change the location of the point of minimum and point of maximum, r_{min} and r_{max} , respectively, of the PEL $V(r)$. Hence, r_{min} and r_{max} coincide with the minimum and maximum (separated by the cage barrier) of $V(r)$. Furthermore, from the Stokes friction formula, we have: $b = 6\pi\mu_0 a$, where μ_0 is the liquid viscosity in the limit of zero shear rate and a is the molecular radius. Upon replacing in the above formula, we finally obtain:

$$\tau = \tau_{\dot{\gamma}=0} e^{-\mu_0 \dot{\gamma} a \Delta r^2 / k_B T}, \quad (13)$$

where we identified $\tau_{\dot{\gamma}=0} = \frac{2\pi b \exp[\beta V(r_{\text{max}}) - \beta V(r_{\text{min}})]}{\sqrt{-V''(r_{\text{max}})V''(r_{\text{min}})}}$ as the barrier crossing time-scale in the absence of shear. We notice that the argument of the exponential in Eq. (13) is, correctly, dimensionless. Since $\Delta r \sim 4a$, the

argument of the exponential is a number very close to the particle Peclet number, i.e. $Pe \equiv 6\pi\mu_0 \dot{\gamma} a^3 / k_B T$. Upon substituting in Eq. (3), we get the following expression for the effective diffusivity:

$$D_{\text{eff}} = \frac{\delta^2}{6\tau} = \frac{\delta^2}{6\tau_{\dot{\gamma}=0}} e^{\mu_0 \dot{\gamma} a \Delta r^2 / k_B T} = D e^{\mu_0 \dot{\gamma} a \Delta r^2 / k_B T}. \quad (14)$$

For molecular liquids, the molecule Peclet number is a small number, much smaller than 1, and therefore we can Taylor expand about $\dot{\gamma} = 0$, to get

$$D_{\text{eff}} = D \left(1 + \frac{\mu_0 a \Delta r^2}{k_B T} \dot{\gamma} \right) \quad (15)$$

which thus recovers the empirical form Eq. (2) observed in simulations and experiments [3–5] and thus identifies the prefactor as

$$c = \frac{\mu_0 a \Delta r^2}{k_B T}. \quad (16)$$

Equation (15) is the most important result of this paper, which provides the missing link between effective diffusivity, shear rate, viscosity, molecular size, and temperature in sheared supercooled liquids.

We can now verify the above theoretical predictions in comparison with numerical simulations. To this aim we performed nonequilibrium molecular dynamics (NEMD) simulations with two very different liquids, i.e. water and the Lennard-Jones (LJ) liquid. In the NEMD, the SLLOD equations of motion were used [24] with Lees-Edwards periodic boundary conditions. A multi-step equilibration procedure was applied in the supercooled regime as described with full details in previous work [3, 4]. The 2D self-diffusion coefficient D_{eff} was calculated by taking ensemble averages over all molecules and time origins in the y and z dimensions, for shear applied in the xy plane. The viscosity was calculated by dividing the average stress by the shear rate $\dot{\gamma}$. Diffusivity and viscosity were calculated by averaging data from 5 independent trajectories. Furthermore, the NEMD simulations were validated by analyzing the velocity profile in the sheared xy -plane.

For supercooled water, the mW molecular model has been used [25]. Simulations with $N = 4096$ molecules were carried out in the temperature range $T = 235 - 260\text{K}$ and in a broad range of shear rates $\dot{\gamma} = 0.001 - 0.75$, in units of reciprocal simulation time.

The effective diffusivity D_{eff} was found to perfectly follow the linear dependence on the shear rate $\dot{\gamma}$ given by Eq. (2), as shown in previous work [3, 4] and in the Supplementary Material therein. From the linear fit, the coefficient c was extracted for different conditions of temperature T and of the zero shear viscosity μ_0 . The results are shown in Fig. 2 and fully support the analytical result derived in Eq. (15).

We used the same protocol for the LJ liquid, with $N = 4096$, temperature (ϵ/k_B) in the range $0.55 - 0.7$ and

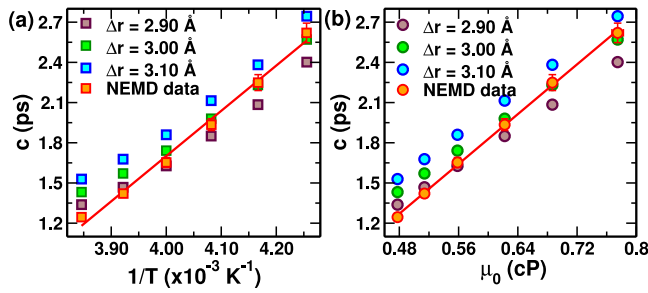


Figure 2. Symbols are the values of prefactor c in $D_{\text{eff}} = D(1 + c\dot{\gamma})$ of supercooled mW water, plotted as a function of temperature T in panel (a) and as a function of the zero shear viscosity μ_0 in panel (b). The maroon, green, and blue symbols show the theoretical predictions using Eq. (16), whereas the red symbols show the NEMD simulation data, respectively. Solid red lines are linear fit to the NEMD simulation data.

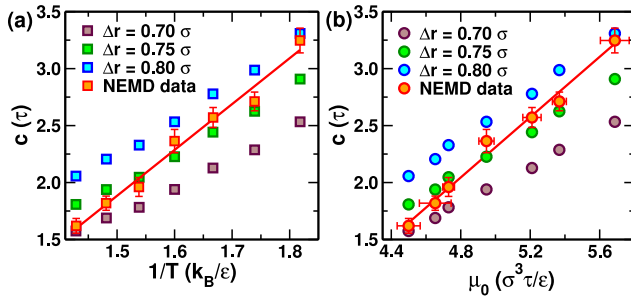


Figure 3. Symbols are the values of prefactor c in $D_{\text{eff}} = D(1 + c\dot{\gamma})$ of supercooled LJ particles, plotted as a function of temperature T in panel (a) and as a function of the zero shear viscosity μ_0 in panel (b). The maroon, green, and blue symbols show the theoretical predictions using Eq. (16), whereas the red symbols show the NEMD simulation data, respectively. Solid red lines are linear fit to the NEMD simulation data.

shear rate in the range $0.001 - 0.5$ (both in LJ units, with ϵ the LJ energy scale and τ the LJ time scale). Also in this case, simulations data were found to follow Eq. (2) perfectly in previous work already [3, 4]. Here, again, we analyzed the behaviour of the prefactor c as a function of temperature and zero shear viscosity. The results are shown in Fig. 3.

Also in this case, the simulation results fully confirm the validity of Eq. (15) for both the predicted dependencies of D_{eff} on temperature T and on the zero shear viscosity μ_0 .

In summary, we have presented the first theory of effective diffusion in shear flows valid for supercooled liquids and we validated the theoretical predictions of

the shear-induced self-diffusion enhancement by means of nonequilibrium molecular dynamics simulations for two very different fluids. The enhancement of self-diffusion of a tracer molecule in an equilibrium (non-supercooled) liquid is well understood thanks to the Taylor-Aris dispersion theory [1, 2], which predicts an enhancement of diffusivity proportional to the square of the Peclet number. The Taylor-Aris theory is based on solving the governing convection-diffusion equation in the absence of any force fields to represent the local potential energy landscape. This assumption is no longer tenable in the supercooled regime, where molecular crowding leads to transient caging effects. These, in turn, represent an energy barrier to the diffusive thermal hopping. Hence, the problem has been reformulated in terms of the Smoluchowski diffusion equation with shear flow and with a mean-force potential that represents the molecular crowding. The equation has been solved analytically for the steady-state current using the Kramers' escape theory and combining this result with Frenkel's theory of diffusivity leads to a shear-induced effective self-diffusion coefficient given by Eq. (15).

Contrary to the Taylor-Aris result, the shear-induced enhancement of self-diffusion in the supercooled regime is now only linear in the shear rate, instead of quadratic. Furthermore, the enhancement is proportional to the zero shear viscosity and inversely proportional to temperature. Both these dependencies predicted by the theory are successfully and quantitatively confirmed in comparison with nonequilibrium molecular simulations of supercooled water and of the supercooled Lennard-Jones liquid. This hints at the possible universality of the phenomenon, and explains previous experimental observations of shear diffusion in hard-sphere colloidal glass [5]. Future extensions of this theory can address the cross-over from supercooled to equilibrium liquid upon increasing T , where the Kramers escape theory has to be modified to recover free diffusion [26]. All in all, given the technological importance of supercooled liquids, these results are expected to be transformational for the quantitative modelling and rational control of mass transfer and molecular and colloidal transport phenomena in a variety of physico-chemical systems [27–30].

Acknowledgments

A.Z. gratefully acknowledges funding from the European Union through Horizon Europe ERC Grant number: 101043968 “Multimech”, and from US Army Research Office through contract nr. W911NF-22-2-0256. M.B. and J.K.S. thank the HPC and NSM supercomputing facilities of Indian Institute of Technology, Kanpur, for providing the computational resources.

- [2] R. Aris and G. I. Taylor, *Proceedings of the Royal Society of London. Series A. Mathematical and Physical Sciences* **235**, 67 (1956).
- [3] A. Goswami, I. S. Dalal, and J. K. Singh, *Phys. Rev. Lett.* **126**, 195702 (2021).
- [4] S. Srirangam, M. Bhendale, and J. K. Singh, *Phys. Chem. Chem. Phys.* **25**, 21528 (2023).
- [5] C. Eisenmann, C. Kim, J. Mattsson, and D. A. Weitz, *Phys. Rev. Lett.* **104**, 035502 (2010).
- [6] D. J. Evans and G. Morriss, *Statistical Mechanics of Nonequilibrium Liquids*, 2nd ed. (Cambridge University Press, 2008).
- [7] J. Frenkel, *Kinetic Theory of Liquids*, Oxford University Press (Oxford, 1955).
- [8] J. C. Dyre, *Journal of Non-Crystalline Solids* **235-237**, 142 (1998).
- [9] J. Krausser, K. H. Samwer, and A. Zaccone, *Proceedings of the National Academy of Sciences* **112**, 13762 (2015).
- [10] A. D. Phan and K. S. Schweizer, *The Journal of Physical Chemistry B* **122**, 8451 (2018), pMID: 30091919, <https://doi.org/10.1021/acs.jpcc.8b04975>.
- [11] M. Fuchs and M. E. Cates, *Phys. Rev. Lett.* **89**, 248304 (2002).
- [12] A. Zaccone, *Theory of Disordered Solids* (Springer, Heidelberg, 2023).
- [13] A. Zaccone and E. M. Terentjev, *Phys. Rev. E* **85**, 061202 (2012).
- [14] W. B. Russel, D. A. Saville, and W. R. Schowalter, *Colloidal Dispersions*, Cambridge Monographs on Mechanics (Cambridge University Press, 1989).
- [15] J. K. Dhont, *An introduction to dynamics of colloids* (Elsevier, 1996).
- [16] A. Zaccone, H. Wu, D. Gentili, and M. Morbidelli, *Phys. Rev. E* **80**, 051404 (2009).
- [17] S. Riva, L. Banetta, and A. Zaccone, *Phys. Rev. E* **105**, 054606 (2022).
- [18] B. O. Conchúir and A. Zaccone, *Phys. Rev. E* **87**, 032310 (2013).
- [19] P. Hänggi, P. Talkner, and M. Borkovec, *Rev. Mod. Phys.* **62**, 251 (1990).
- [20] A. Zaccone and E. M. Terentjev, *Phys. Rev. Lett.* **108**, 038302 (2012).
- [21] H. Kramers, *Physica* **7**, 284 (1940).
- [22] C. Ness and A. Zaccone, *Industrial & Engineering Chemistry Research* **56**, 3726 (2017), <https://doi.org/10.1021/acs.iecr.7b00337>.
- [23] A. Nitzan, *Chemical dynamics in condensed phases* (Oxford University Press, New York, N.Y., 2013).
- [24] P. J. Daivis and B. D. Todd, *The Journal of Chemical Physics* **124**, 194103 (2006), <https://pubs.aip.org/aip/jcp/article-pdf/doi/10.1063/1.2192775/13451972/194103-1.online.pdf>.
- [25] V. Molinero and E. B. Moore, *The Journal of Physical Chemistry B* **113**, 4008 (2009), pMID: 18956896, <https://doi.org/10.1021/jp805227c>.
- [26] M. Abkenar, T. H. Gray, and A. Zaccone, *Phys. Rev. E* **95**, 042413 (2017).
- [27] B. A. Grzybowski, Y. I. Sobolev, O. Cybulski, and B. Mikulak-Klucznik, *Nature Reviews Materials* **7**, 338 (2022).
- [28] H. Wu, A. Zaccone, A. Tsoutsoura, M. Lattuada, and M. Morbidelli, *Langmuir* **25**, 4715 (2009), pMID: 19260654, <https://doi.org/10.1021/la803789s>.
- [29] H. Wu, A. Tsoutsoura, M. Lattuada, A. Zaccone, and M. Morbidelli, *Langmuir* **26**, 2761 (2010), pMID: 19845347, <https://doi.org/10.1021/la902800x>.
- [30] R. Debuysschère, B. Rimez, A. Zaccone, and B. Scheid, *Crystal Growth & Design* **23**, 4979 (2023), <https://doi.org/10.1021/acs.cgd.3c00232>.